Supplement of Atmos. Chem. Phys., 25, 10293–10314, 2025
https://doi.org/10.5194/acp-25-10293-2025-supplement

Atmospheric Chemistry and Physics
Open Access

Supplement of

Incorporation of multi-phase halogen chemistry into the Community Multiscale Air Quality (CMAQ) model

Kiyeon Kim et al.

Correspondence to: Chul Han Song (chsong@gist.ac.kr)

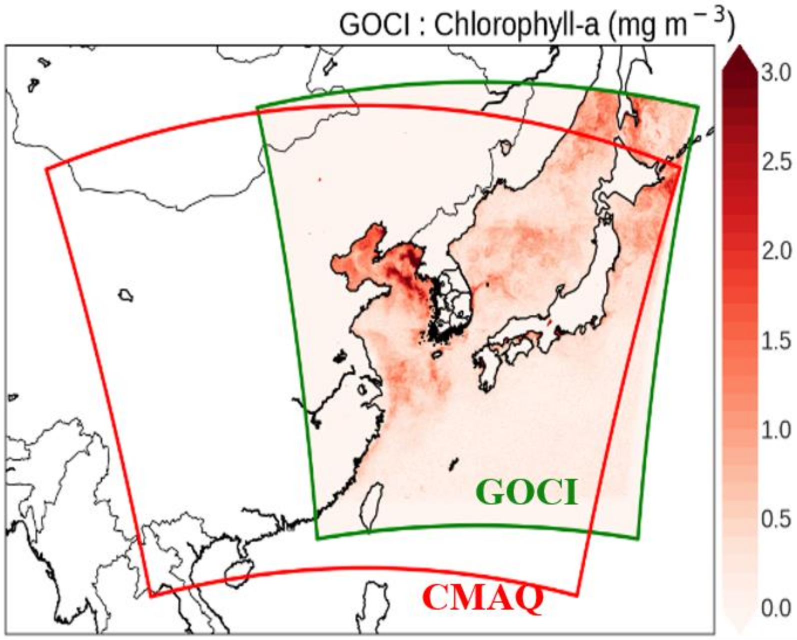

Fig. S1. Map of Chlorophyll-a concentrations obtained from GOCI satellite sensors over East Asia. The red and green lines represent domain of CMAQ model and GOCI sensor, respectively.

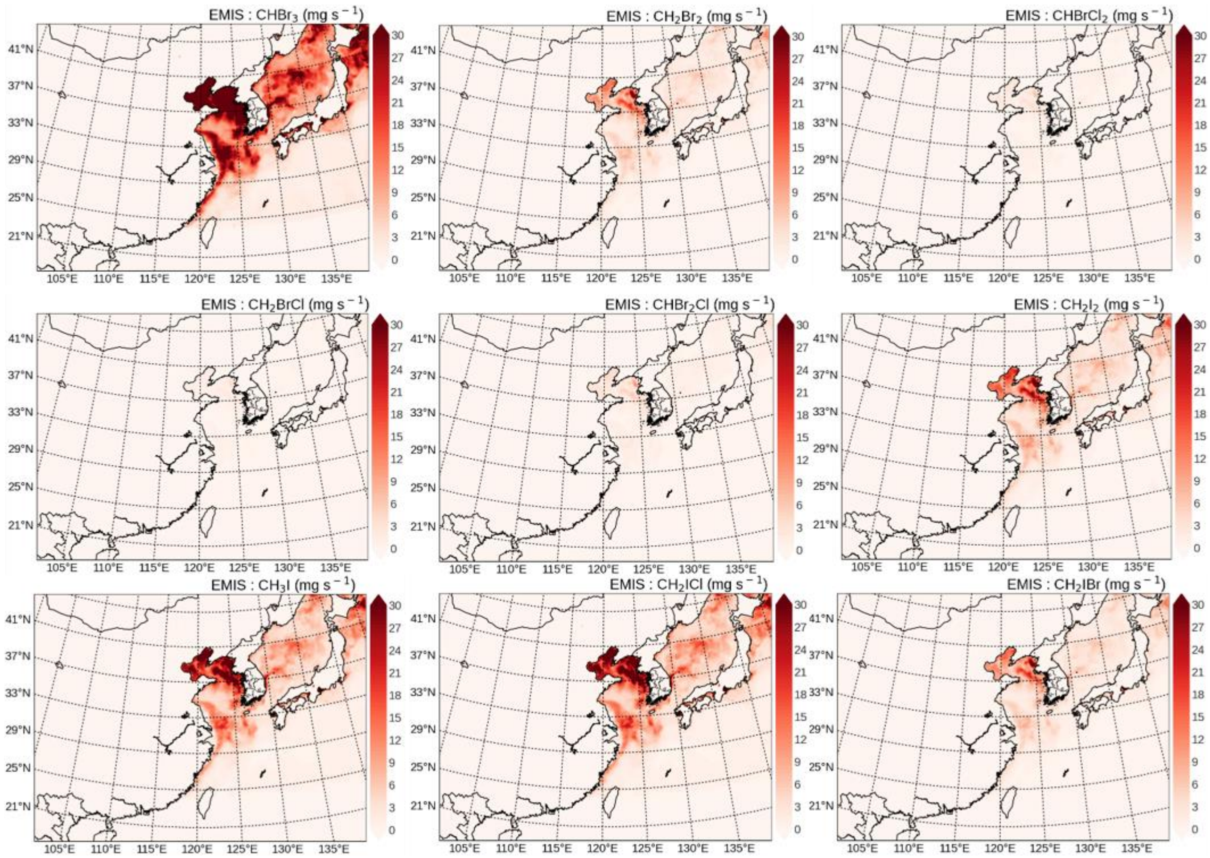

Fig. S2. Spatial distributions of GOCI-driven halocarbon emission rates across East Asia.

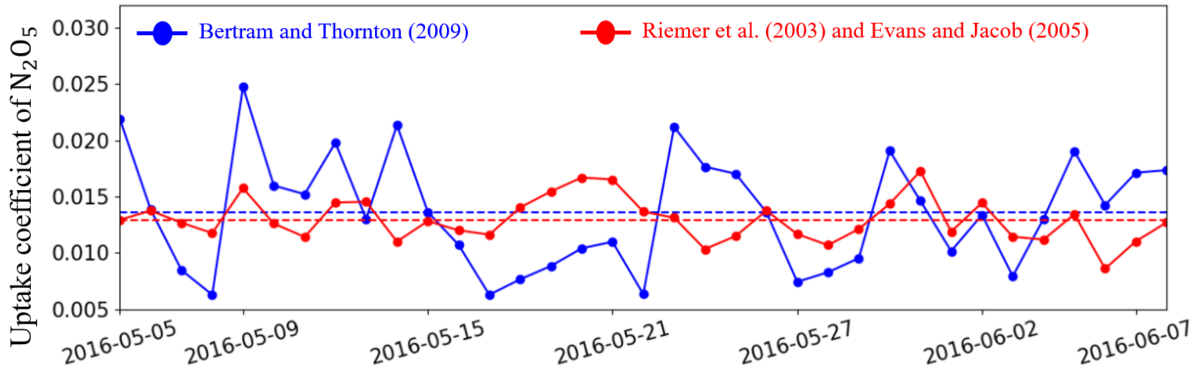

Fig. S3. The blue and red solid lines represent the temporal variations in the uptake coefficients of N_2O_5 based on Bertram and Thornton (2009) and Riemer et al. (2003) combined with Evans and Jacob (2005), respectively. The horizontal dotted lines show the averaged $\boldsymbol{\gamma_{N2O5}}$ over the period of KORUS-AQ campaign (average of blue dotted line is equal to 0.0135 and average of red dotted line is 0.0129).

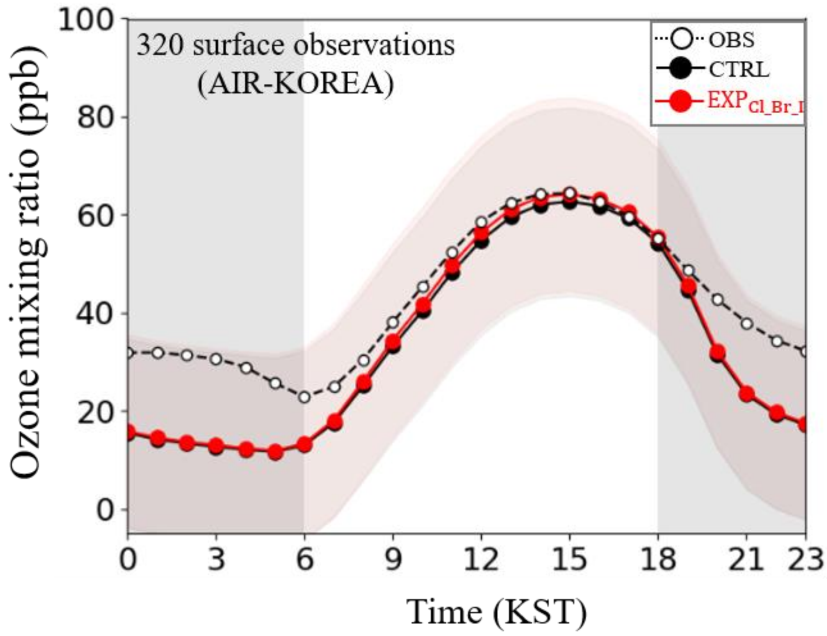

Fig. S4. Comparison of diurnal variations in O_3 mixing ratios at 320 AIR-KOREA monitoring stations during the period of the KORUS-AQ campaign. The white open circles, black and red lines represent observed mixing ratios and modeled mixing ratios from the CTRL and $EXP_{Cl\_Br\_I}$ simulations, respectively.

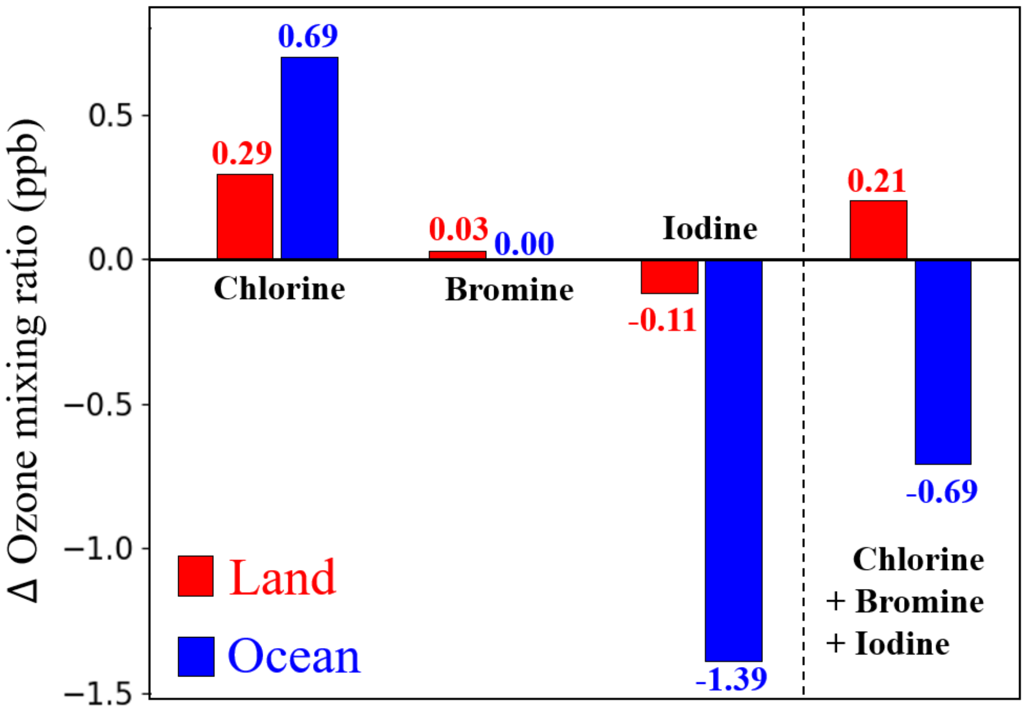

Fig. S5. The impacts of halogen chemistry on the changes of O_3 mixing ratios over land (represented by red bars) and ocean (represented by blue bars) between the CTRL and $EXP_{Cl\_Br\_I}$ simulations.

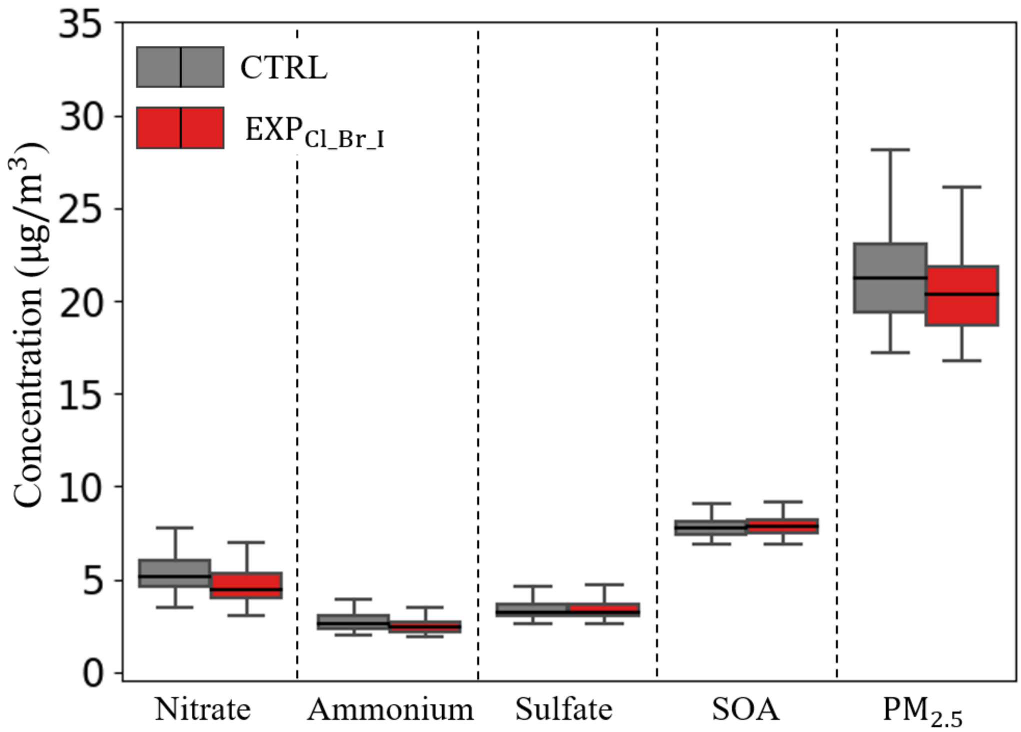

Fig. S6. Box plots represent the average concentrations of particulate species such as nitrate, ammonium, sulfate, secondary organic aerosol (SOA), and particulate matter ($PM_{2.5}$) in the CTRL and $EXP_{Cl\_Br\_I}$ simulations over Korean peninsula. The whisker marks exhibit ranges from the lower quartile (25%) – 1.5×IQR to the upper quartile (75%) + 1.5×IQR, where IQR is the difference between the upper and lower quartiles.

Table S1. List of WRF model configurations used in our study.

WRF v3.8.1		
Microphysics	Parameterization scheme	Reference
Cumulus Parameterization	Grell-Freitas	Grell and Freitas et al. (2014)
PBL Scheme	Yonsei University	Hong et al. (2006)
Shortwave & Longwave	RRTMG Scheme	Iacono et al. (2008)
Land Surface Scheme	NOAH Land Surface Model	Chen and Dudhia (2001)
Surface Layer Scheme	Revised MM5 (Jimenez)	Jimenez et al. (2012)
Cloud Microphysics	WRF Single Moment 3 Class (WSM3)	Hong et al. (2004)

Table S2. Comparison of updated halogen reactions between EXP_{CMAQ} and this study.

	Reaction	EXP_{CMAQ}	This study ($EXP_{Cl\_Br\_I}$)	Ref.
R20 in Table 1	$ClO + ClO \xrightarrow{k_1} 0.29Cl_2 + 1.42Cl$	$ClO + ClO \xrightarrow{k_1} 0.29Cl_2 + 1.42Cl$ $k_1 = 1.25 \times 10^{-11} e^{-1960/T}$	$ClO + ClO \xrightarrow{k_1} Cl_2$ $k_1 = 1.0 \times 10^{-12} e^{-1590/T}$	1
R8 in Table 3	$HOBr(g) + Cl^-(aq) \xrightarrow{\gamma_{HOBr}} BrCl(g)$	-	$\gamma_{HOBr} = 0.02$	2
R1 in Table 3	$N_2O_5(g) + (1\text{-}\varphi)H_2O + \varphi Cl^-(aq) \xrightarrow{\gamma_{N2O5}} (2\text{-}\varphi)HNO_3(aq) + \varphi ClNO_2\ (g)$	$\gamma_{N_2O_5} = 3.2 \times 10^{-8} k \frac{1}{\left(\frac{0.06[H_2O](l)}{[NO_3^-]}\right)+1+\left(\frac{29[Cl^-]}{[NO_3^-]}\right)}$ $k = 1.15 \times 10^6 - 1.15 \times 10^6 e^{[-0.13x[H_2O(l)]}$	$\gamma_{N_2O_5} = f \times \gamma_1 + (1 - f) \times \gamma_2$ $f = \frac{m_{SO_4^{2-}}}{m_{SO_4^{2-}} + m_{NO_3^-}}$ where m_X represents the aerosol mass concentration of the species $\gamma_1 = \alpha \times 10^{\beta}$ $\gamma_2 = 0.1 \times \gamma_1$ $\alpha = 2.79 \times 10^{-4} + 1.3 \times 10^{-4} \times RH - 3.43 \times 10^{-6} \times RH^2 + 7.52 \times 10^{-8} \times RH^3$ $\beta = 0.48\ (T < 282K)$ $\beta = 4 \times 10^{-2} \times (294 - T)\ (T \geq 282K)$	3,4,5
R6 in Table 3	$2NO_2(g) + Cl^-(aq) \xrightarrow{\gamma_{NO2}} ClNO(g) + NO_3^-\ (aq)$	-	$\gamma_{NO2} = 10^{-4}$	6

1. Burkholder et al. (2020); 2. Fernandez et al. (2014); 3. Bertram and Thornton (2009); 4. Riemer et al. (2003); 5. Evans and Jacob (2005) 6. Abbatt and Waschewsky et al. (1998)

References

Abbatt, J. and Waschewsky, G.: Heterogeneous interactions of HOBr, HNO3, O3, and NO2 with deliquescent NaCl aerosols at room temperature, J. Phys. Chem. A, 102, 3719-3725, https://doi.org/10.1021/jp980932d, 1998.

Bertram, T. and Thornton, J.: Toward a general parameterization of N2O5 reactivity on aqueous particles: the competing effects of particle liquid water, nitrate and chloride, Atmos. Chem. Phys., 9, 8351-8363, https://doi.org/10.5194/acp-9-8351-2009, 2009.

Burkholder, J., Sander, S., Abbatt, J., Barker, J., Cappa, C., Crounse, J., Dibble, T., Huie, R., Kolb, C., and Kurylo, M.: Chemical kinetics and photochemical data for use in atmospheric studies; evaluation number 19, Nasa panel for data evaluation technical report, 19-5, https://jpldataeval.jpl.nasa.gov/pdf/NASA-JPL%20Evaluation%2019-5.pdf, 2020.

Chen, F. and Dudhia, J.: Coupling an advanced land surface–hydrology model with the Penn State–NCAR MM5 modeling system. Part I: Model implementation and sensitivity, Monthly weather review, 129, 569-585, https://doi.org/10.1175/1520-0493(2001)129<0569:CAALSH>2.0.CO;2, 2001.

Evans, M. J. and Jacob, D. J.: Impact of new laboratory studies of N2O5 hydrolysis on global model budgets of tropospheric nitrogen oxides, ozone, and OH, Geophys. Res. Lett., 32, https://doi.org/10.1029/2005GL022469, 2005.

Fernandez, R. P., Salawitch, R., Kinnison, D. E., Lamarque, J.-F., and Saiz-Lopez, A.: Bromine partitioning in the tropical tropopause layer: implications for stratospheric injection, Atmos. Chem. Phys., 14, 13391-13410, https://doi.org/10.5194/acp-14-13391-2014, 2014.

Grell, G. A. and Freitas, S. R.: A scale and aerosol aware stochastic convective parameterization for weather and air quality modeling, Atmos. Chem. Phys., 14, 5233-5250, https://doi.org/10.5194/acp-14-5233-2014, 2014.

Hong, S.-Y., Dudhia, J., and Chen, S.-H.: A revised approach to ice microphysical processes for the bulk parameterization of clouds and precipitation, Monthly weather review, 132, 103-120, https://doi.org/10.1175/1520-0493(2004)132<0103:ARATIM>2.0.CO;2, 2004.

Hong, S.-Y., Noh, Y., and Dudhia, J.: A new vertical diffusion package with an explicit treatment of entrainment processes, Monthly weather review, 134, 2318-2341, https://doi.org/10.1175/MWR3199.1, 2006.

Iacono, M. J., Delamere, J. S., Mlawer, E. J., Shephard, M. W., Clough, S. A., and Collins, W. D.: Radiative forcing by long-lived greenhouse gases: Calculations with the AER radiative transfer models, J. Geophys. Res., 113, https://doi.org/10.1029/2008JD009944, 2008.

Jiménez, P. A., Dudhia, J., González-Rouco, J. F., Navarro, J., Montávez, J. P., and García-Bustamante, E.: A revised scheme for the WRF surface layer formulation, Monthly weather review, 140, 898-918, https://doi.org/10.1175/MWR-D-11-00056.1, 2012.

Riemer, N., Vogel, H., Vogel, B., Schell, B., Ackermann, I., Kessler, C., and Hass, H.: Impact of the heterogeneous hydrolysis of N2O5 on chemistry and nitrate aerosol formation in the lower troposphere under photosmog conditions, J. Geophys. Res., 108, https://doi.org/10.1029/2002JD002436, 2003.